Improved cardiac wall motion tracking based on harmonic phase technique

Diaa El-Deen M. Yousry[1,2], Abou-Bakr Youssef[1], Mohamed S. El-Sherif[2] and Yasser M. Kadah[1*]
[1]Biomedical Engineering Dept., Cairo University, and [2]Electronics Research Institute, Giza, Egypt

ABSTRACT

The problem of detecting and tracking SPAMM tags has been the focus of cardiac MRI in the past few years. Among the many methods proposed to do that, the harmonic phase method (called HARP) has a large potential to enable real-time tracking. We propose two improvements to the original HARP technique to address the problem of magnetic field inhomogeneity and improve tracking. We derive a theoretical model for the problem of field inhomogeneity and propose an extension of the simulated phase evolution rewinding technique (SPHERE) whereby consecutive images are acquired using alternating echo time. Then, we propose a simple and computationally efficient approach that allows the problems of disappearing tag lines to be addressed. In particular, the geodesic horizontal and vertical distances between neighboring corner points in the detected tag lines are computed for each image. Once the correspondence between tag lines is established, the tracking of any point on the wall can be obtained given its relationship to the four corner points surrounding its location. The proposed improvements were implemented and applied to numerical phantoms as well as experimental data obtained for the original HARP technique to demonstrate the potential of the new techniques.

Keywords: Cardiac MRI, harmonic phase technique, motion tracking, magnetic field inhomogeneity.

1. INTRODUCTION

The development of tagged cardiac magnetic resonance imaging has led to a set of analysis tools that helped in the noninvasive assessment of heart performance[1]. Heart performance can be assessed by measuring the detailed strain patterns of the myocardium. Strain patterns can reflect the normal and abnormal myocardial motion, which can be used to correlate the myocardial motion abnormalities with the coronary artery disease.

In the past few years, several techniques have been developed for fast and accurate tracking of cardiac wall motion. For example, some techniques used multi-frame temporal estimation of cardiac nonrigid motion[2]. The main limitation for this method is that its validation requires implanting physical markers in the left ventricle wall as a reference for comparison with the computed trajectories. Other techniques attempted to fit the tag lines with deformable models that enabled the tracking and strain estimation. Another technique uses phase contrast approaches to MRI motion analysis[3]. Phase contrast is not suitable for point to point tracking in the left ventricular wall due to the noise associated with nonhomoginous material along boundaries.

Among the new developments in cardiac magnetic resonance imaging, the harmonic phase magnetic resonance imaging (HARP) stands out as the technique with the largest potential for clinical use[4]. This method relies on the fact that utilizing spatial modulation of magnetization (SPAMM) tag patterns results in a set of spectral peaks in the k-space. Each spectral peak contains information about a particular component of tissue motion. Motion information can be extracted by observing the phase of the image of one of the spectral peaks (usually the one corresponding to the first harmonic). HARP tracking is based upon tracking the points in the filtered image sequence that have the same phase value and lie within the tag period. The tracked points can be used to calculate both circumferential and radial Lagrangian strain.

Even though fast computation and good experimental results have been reported using the HARP method, a number of theoretical limitations of the technique are yet to be addressed in order to enhance the robustness of its implementation in

* E-mail: ymk@ieee.org

Medical Imaging 2002: Physiology and Function from Multidimensional Images, Anne V. Clough, Chin-Tu Chen, Editors, Proceedings of SPIE Vol. 4683 (2002) © 2002 SPIE · 1605-7422/02/$15.00

the clinical settings. In this paper, we propose two improvements to the original HARP technique to address the problems of magnetic field inhomogeneity and the accuracy of the current point tracking strategy. In particular, we develop a model for the effect of magnetic field inhomogeneity on the accuracy of tag line detection. Then, the problems of point tracking such as disappearance/reappearance of tag lines in the sequence of images are considered and a simple method is proposed to perform the 2-D tracking. The proposed improvements were implemented and applied to numerical phantoms as well as experimental data obtained for the original HARP technique to demonstrate the success of the new techniques. These improvements help the original HARP technique become more robust for practical application.

Once the tag lines are defined, one of the original problems in the original HARP processing is how to map points from one image to next. Here, we propose a simple and computationally efficient approach that allows the problem of disappearing tag lines inside the region of interest to be addressed. Vertical and horizontal tag lines are detected from which we generate a motion grid in which each corner point represents an intersection of vertical and a horizontal tag line. In particular, the geodesic horizontal and vertical distances between neighboring corner points in the motion grid are computed to generate two matrices containing these horizontal and vertical distances indexed by their corner point location and maintaining the topological neighborhood relationships the same (i.e., neighboring corner points occupy consecutive positions in these matrices). Once these matrices are defined, the problem of correspondence becomes a substantially simpler registration problem given the smaller number of corner points compared to image points. The registration process also involves only translational motion in the new space. Given the practical continuity constraints, the location of points providing the minimum Frobenius norm for the error between two consecutive images. This allows the robust handling of the problem of disappearing/reappearing tag lines in the region of interest. Once the correspondence between tag lines is established, the tracking of any point on the wall can be obtained given its relationship to the four corner points surrounding its location.

2. MAGNETIC FIELD INHOMOGENEITY CORRECTION MODEL

2.1 Model

The effect of the magnetic field Inhomogeneity can be observed in two aspects of the imaging procedure, namely, the creation of the SPAMM tags and the geometric/phase distortion of the tag lines. Consequently, these two aspects may affect the results of HARP analysis. Even though the first effect is usually minimal due to the use of large gradients when the SPAMM tagging RF pulses are applied, the second is more complicated and can cause significant errors in tracking the tag lines. Therefore, we focus on this aspect in this work. In particular, we derive a theoretical model for this problem and observe that the problem involves time-varying inhomogeneity distribution as a result of the heart motion. We propose an extension of the simulated phase evolution rewinding technique (SPHERE) whereby consecutive images are acquired using alternating echo time. That is, the echo time in the image sequence switches between TE and TE+Δt where Δt is very small. Using this small difference, an updated field map can be computed for each for each image and is subsequently used to obtain the corrected images that are used for further HARP analysis. Another method for generating the updated field map, which considers each two successive images for generating a common field map that, can be used to obtain the corrected images.

As shown in Figure 1(a) the tagged magnetic resonance image appears intensity-modulated due to the presence of the SPAMM tag lines. This particular type of modulation can be modeled by a truncated cosine series. As the result, the magnitude of the Fourier transform of this image (shown in Figure 1(b)) demonstrates a set of spectral peaks due to the presence of the SPAMM tags. In a mathematical form, the SPAMM-tagged image can be expressed in such a way such that the value of image point at coordinate *y* at time *t* is given by,

$$I(y,t) = \sum_{l=-L}^{l=+L} I_l(y,t) \ . \tag{1}$$

Here, each complex image $I_l(y,t)$ corresponds to a separate spectral peak[6]. In Figure 1(b), it can be seen that there are five spectral peaks, which means that *L*=2. Let ω be the position of the spectral peak closest to the origin. Then, the *l*-th harmonic image can be represented by the following formula that is considered the basis of HARP,

$$I_l(y,t) = D_l(y,t) e^{jl\omega^T q(y,t)}, \tag{2}$$

where $D_l(y,t)$ is called the harmonic magnitude image and $q(y,t)$ is called the apparent reference map. Hence, D_l is a real-valued image that resembles the untagged MR image. Because tagging is done once in the reference frame, D_l fades over the cardiac cycle and finally becoming overwhelmed by noise during diastole. The apparent reference map q gives the apparent position at time 0 (end-diastole) of a material point located at y at time t.

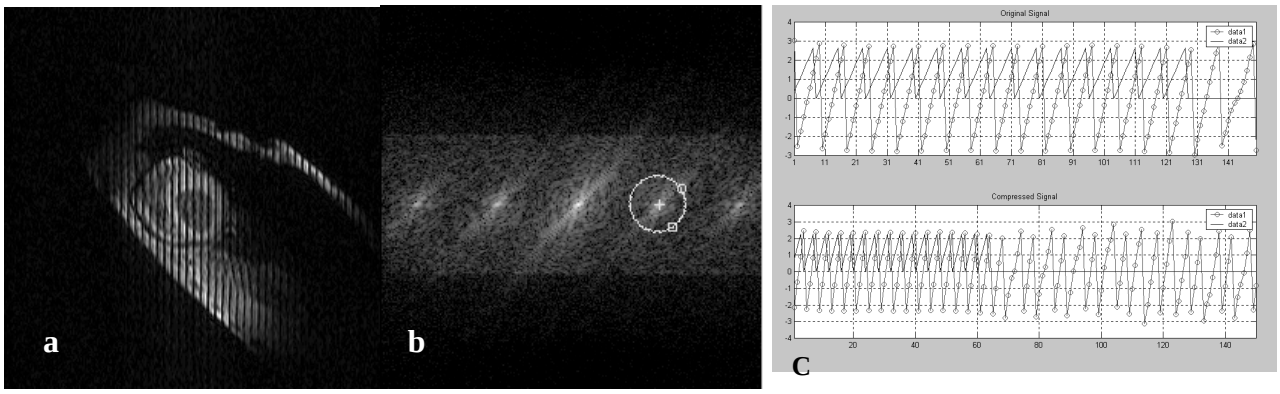

Figure 1. (a) Tagged MR image that appears like a modulated image due to the presence of the SPAMM tag lines and (b) The magnitude of the Fourier transform of this image as showed in showing set of spectral peaks due to the presence of the SPAMM tags (c) Shows the reference harmonic phase signal and its corresponding reference tagged signal, while as well as the effect of change in tag pattern frequency due to cardiac wall motion.

In standard planar tagging, the apparent reference position is precisely the projection of the actual reference position onto the image plane. From (2), it can be seen that the motion described by $q(y,t)$, phase modulates the underlying image. This causes the energy to be spread around the spectral peak $l\omega$ depending on the magnitude of $l\omega$ and the magnitude of the motion. By designing an appropriate band-pass filter, we can isolate a single spectral peak including most of the effects of phase modulation. In HARP tracking only two spectral peaks are used, first-order harmonic from each of the horizontal and vertical tagged images. Here forth, the horizontal and vertical harmonic images will be referred by $I_l(y,t)$, l=1,2. These images are represented mathematically by,

$$I_l(y,t) = D_l(y,t)e^{j\phi_l(y,t)}, \tag{3}$$

where,

$$\phi_l(y,t) = \omega_l^T q(y,t). \tag{4}$$

Here, ω_l, l = 1,2, represents the position of the closest harmonic peaks in the two cases of vertical and horizontal tagging directions. Also, ϕ_l will be called the harmonic phase mage. The two harmonic phase images arising from vertical and horizontal tagging can be written as the vector,

$$\phi(y,t) \equiv [\phi_1(y,t) \quad \phi_2(y,t)]^T. \tag{5}$$

This harmonic phase vector is related to the motion by the compact matrix expression,

$$\phi(y,t) = \Omega^T q(y,t), \tag{6}$$

where,

$$\Omega \equiv [\omega_1 \quad \omega_2]. \tag{7}$$

By using the harmonic phase images, the reference map can by directly computed by inverting Ω. Unfortunately, only the wrapped version of the harmonic phase images can be computed due to the use of arctangent of the ratio of the

imaginary to the real parts. The relationship between the wrapped harmonic phase vector a and ϕ is given by the formula,

$$a = W(\phi), \tag{8}$$

where,

$$W(\phi) = mod(\phi + \pi, 2\pi) - \pi \quad . \tag{9}$$

The main difficulty in the harmonic phase imaging is dealing with the wrapping effect. That is why the cardiac wall motion tracking makes use of the slope of the phase not the phase itself. Local phase unwrapping can be calculated at the points of phase discontinuity to correct the slope at these points. The idea of HARP can be illustrated using one-dimensional example as shown in Figure 1 (c) where the reference harmonic phase signal and its corresponding reference tagged signal as well as the effect of changing the tag pattern frequency due to cardiac wall motion. When the tag pattern frequency decreases the slope of phase in the reference map also decreases. It can be noticed that the change in the slope of the phase is directly related to the change in the tag pattern from which we can use phase in point tracking. Once cardiac wall points are tracked radial and circumferencial lagrangian strain can be calculated[4].

2.2 HARP tracking

As shown in Figure 1 (b) the Fourier transform of a SPAMM tagged image shows a set of spectral peaks. HARP imaging requires a band pass filter to extract the first harmonic in the Fourier domain centered on frequency ω. Generally we use elliptic band pass filter with smooth extent to extract this spectral peak. Once the band pass filter has been designed it is used for the whole image set of the same tagging direction. By applying the inverse Fourier transform we can get the image described by,

$$I_l(y,t) = D_l(y,t)e^{j\phi_l(y,t)}. \tag{10}$$

The harmonic phase image $\phi_l(y,t)$ carries the motion information of the cardiac wall, which was simply illustrated in the one-dimensional example shown in Figure 1 (c). When the tag pattern frequency decreased the slope of phase in the reference map decreased. It can be noticed that the change in the slope of the phase is directly related to the change in the tag pattern from which we can use phase in point tracking. Since the HARP phase of material point remains constant as it moves, then we can write,

$$\frac{d\phi(y,t)}{dt} = 0. \tag{11}$$

This formula can be rewritten using chain rule as,

$$\nabla\phi(y,t)v(y,t) + \frac{\partial\phi}{\partial t} = 0 \quad , \tag{12}$$

where ∇ is the gradient with respect to y and $v(y, t)$ is the velocity field at time t. Solving for v yields,

$$v(y,t) = -[\nabla\phi(y,t)]^{-1}\frac{\partial\phi}{\partial t}. \tag{13}$$

As we previously mentioned that it is not easy to calculate ϕ because we have only a its wrapped version. The spatial derivative of ϕ can be calculated directly by differentiating a except at wrapping points of a, so

$$\nabla\phi = \nabla^* a \equiv \begin{bmatrix} \nabla^* a_1 \\ \nabla^* a_2 \end{bmatrix}. \tag{14}$$

Here a_1 and a_2 are the harmonic phase images derived from the vertically and horizontally tagged images respectively.

$$\nabla^* a_l = \begin{cases} \nabla a_l & ||\nabla a_l|| \le ||\nabla W(a_l + \pi)|| \\ \nabla W(a_l + \pi) & otherwise \end{cases} \quad . \tag{15}$$

For l = 1,2 finite difference can be used to calculate the gradient operators. Then the derivative of ϕ can be calculated using the finite derivative of a in successive frames in the CINE sequence. The partial derivative of ϕ with respect to t an be approximated by the following equation,

$$\frac{d\phi(y,t_n)}{dt} \approx \frac{1}{\Delta t} W\left[a(y,t_{n+1}) - a(y,t_n)\right], \tag{16}$$

where Δt is the time separation between to images acquired at t_n and t_{n+1}. This expression is valid for $|\phi(y,t_{n+1}) - \phi(y,t_n)| < \pi$, which is guaranteed if Δt is sufficiently small. Similarly, the velocity vector can be calculated by,

$$v(y,t_n) = \frac{y_{n+1} - y_n}{\Delta t} = -\frac{1}{\Delta t} \nabla^* a^{-1}(y,t) W\left[a(y,t_{n+1}) - a(y,t_n)\right]. \tag{17}$$

Finally we can calculate the new position of y in the next frame by the following equation,

$$y_{n+1} = y_n - \begin{bmatrix} \nabla^* a_1(y_n,t_{n+1}) \\ \nabla^* a_2(y_n,t_{n+1}) \end{bmatrix}^{-1} \begin{bmatrix} W[a_1(y_n,t_{n+1}) - a_1(y_n,t_n)] \\ W[a_2(y_n,t_{n+1}) - a_2(y_n,t_n)] \end{bmatrix}. \tag{18}$$

Computationally, we can use the previous equation for HARP tracking. For tracking a point y_n in the reference frame, y_n will be used as an initial estimate for the tracked points in the successive frames and iteratively y_{n+1} is updated until the vector representing $\frac{d\phi(y,t_n)}{dt}$ approaches a minimum value near zero.

3. MOTION GRID REGISTRATION MODEL

3.1 Model

In this section, we introduce a simple and computationally efficient cardiac wall tracking model. This model assumes the prior detection of vertical and horizontal tag lines from which a motion grid is constructed. The corner points on such grid represent the intersections of vertical and horizontal tag lines. The geodesic horizontal and vertical distances between neighboring corner points are measured and two matrices containing these distances indexed by their corner point locations are constructed. These matrices maintain the topological neighborhood between corner points in such a way that neighboring corner points occupy consecutive positions in these matrices. Once these matrices are calculated for every image in the sequence, applying a simple registration technique between these matrices and the ones from the successive grid enables the detection of correspondence between such corner points. In particular, each corner point in the motion grid will be associated with another point in the successive grid, which is considered the tracked point in the successive frame. As an example, this strategy is applied on a simulated motion grid as shown in Figure 2. Figure 2 (a) shows a motion grid of 33x33 corner points that resembles the number of tag lines found in the typical data sets acquired in SPAMM-tagged cardiac MRI. The square in Figure 2 (a) represents the selected ROI in the image that will be used for tracking the entire grid. The two images showed in Figure 2 (b) and Figure 2 (c) represent the two generated matrices representing the vertical and the horizontal geodesic distances respectively. Hence, corner point tracking is transformed into a 2-D registration of a sequence of these two images obtained from the acquired HARP data set. The tracking of any other general point in the SPAMM-tagged image can be performed using its relation to the surrounding four corner points.

3.2 Motion grid registration

In this part, we use simulated motion grids representing the tag lines in the cardiac tagged MR images. The generated reference motion grid has to be a nonuniform grid. This is because the uniform grid yields a distance image with a constant value, which does not carry a special pattern that can be used in registration. In order to generate a non-uniform motion grid we induced a minute displacement at each grid point scaled by a factor β and in the direction of the unit vector from the center of the grid to that point. Any point $p(i,j)$ located at indexes i and j in the grid will be located in the x-y plane by the following formula,

$$p(i,j) = \begin{bmatrix} x(i) \\ y(j) \end{bmatrix} = \beta \begin{bmatrix} i + \hat{v}_x(i) \\ j + \hat{v}_y(j) \end{bmatrix}, \tag{19}$$

Where $\hat{v}_x$ and $\hat{v}_y$ are the *x* and *y* components of the unit vector from the center of the grid to that point. The vector $\hat{v}(i,j)$ can be defined by the following formula,

$$v(i,j)=\begin{bmatrix}\hat{v}_x(i)\\ \hat{v}_y(j)\end{bmatrix}=\begin{bmatrix}\dfrac{i-c_x}{n(i,j)}\\ \dfrac{j-c_y}{n(i,j)}\end{bmatrix}, \tag{20}$$

where (c_x,c_y) is the center point of the motion grid, which represents the position of distance peak according to the proposed model. $n(i,j)$ is the Euclidean distance from the center point and the point located at the i and j indexes. $n(i,j)$ can be defined by the formula,

$$n(i,j)=\begin{cases}1 & ,\sqrt{(i-c_x)^2+(j-c_y)^2}=0\\ \sqrt{(i-c_x)^2+(j-c_y)^2} & ,otherwise\end{cases}. \tag{21}$$

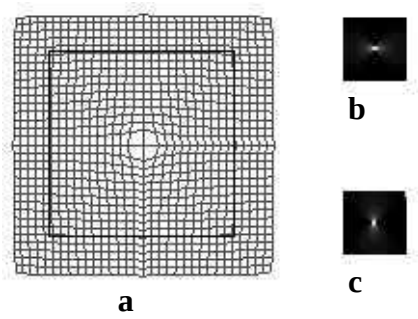

Figure 2. (a) Generated motion grid with the associated ROI. (b) Vertical distance image. (c) Horizontal distance image.

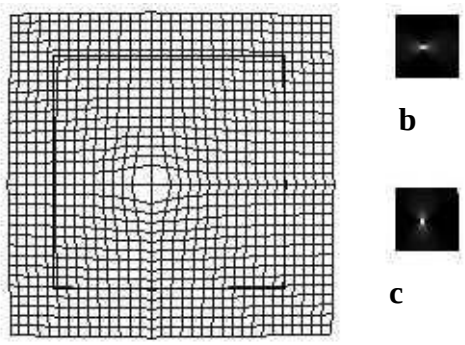

Figure. 3. (a) Generated motion grid resembling cardiac wall motion with the associated ROI. $(c_x,c_y)=(34,28)$ and β =4. (b) Vertical distance image. (c) Horizontal distance image.

The motion grid generated in Figure 2 (a) is a 33×33 motion grid with $(c_x,c_y)=(31,31)$ and β =5. By changing the model parameters ((c_x,c_y) and β), we can generate a set of motion grids that simulates the cardiac wall motion. Figure 3 shows the generated motion grid that modeled the cardiac wall motion. We changed the model parameters to get the motion effect by changing (c_x,c_y) and β. From the generated motion grid we can notice set of points. First, due to changing the (c_x,c_y)-which simulates the transnational motion- set of tag lines got out from the ROI while others got in. Second, we can see that β affected the scaling of the motion grid, which simulates relaxation or contraction of the cardiac muscles.

In order to get exact point matching between the reference frame and the frame of question we have to register the two motion grids lying inside the ROI. Motion grid registration can be accomplished by determining the position (i, j) at which the ROI in the frame of question has to be shifted to it in order to get the minimum RMS error. This position can be determined using the following minimization procedure,

$$P = (i, j) : min_{i,j}[e(i, j)] \forall i : -3 < i < 3, i \in z, \forall j : -3 < j < 3, j \in z . \quad (22)$$

Here e(i, j) is the error due to difference in horizontal and vertical distances. This error is calculated between the ROI in the reference frame and the ROI in the subsequent frame after shifting its index values by *i* in the x-direction and *j* in the y-direction. The error function can be defined by the following formula,

$$e(i, j) = \sqrt{e_v(i, j) + e_h(i, j)} \quad , \quad (23)$$

where $e_v(i, j)$ and $e_h(i, j)$ represents the error in distances between the reference frame and the frame of question in the vertical and horizontal distance matrices respectively. Both $e_v(i, j)$ and $e_h(i, j)$ can be calculated by the following formulas,

$$e_v(i, j) = \frac{1}{N} \sum_{x=t}^{b} \sum_{y=l}^{r} \left[D_v(x + i, y + j) - D_{vref}(x, y) \right]^2 , \quad (24)$$

and

$$e_h(i, j) = \frac{1}{N} \sum_{x=t}^{b} \sum_{y=l}^{r} \left[D_h(x + i, y + j) - D_{href}(x, y) \right]^2 . \quad (25)$$

Here N is the number of points in the ROI of the reference frame. D_v and D_{vref} are the Euclidean distances between the indexed point and the point on their right side in the frame of question and the reference frame respectively. D_h and D_{href} are the Euclidean distances between the indexed point and the point on their bottom side in the frame of question and the reference frame respectively. The $l,t,r,$ and b represent the left, top, right, and bottom coordinates for the ROI respectively.

4. EXPERIMENTAL VERIFICATION

This implementation requires a sequence of SPAMM-tagged magnetic resonance images for complete tracking through the cardiac cycle. This sequence of images is divided into two image sets representing the horizontal and vertical tagging. This is done such that each image in a set (e.g., vertical tagging set) must have a corresponding image in the other set (e.g., horizontal tagging set) that is acquired at the same time instance in the cardiac cycle. Each set will be used in the analysis to compute the motion component in its tagging direction. We used experimental data obtained for the original HARP technique to demonstrate the potential of the new tracking technique[4]. To show the effect of magnetic field inhomogeneity on tracking, we simulated the inhomogeneity artifact on the image set by generating a smooth field map with a 2-D Gaussian shape. We applied the SPHERE[7] technique with a reversed phase sign in order to induce inhomogeneity distortion into the image sequence. In practical applications, this field map will be calculated from each two successive images in each image set with alternating small echo time shift. The simulated field map was generated in such a way to make sure that it is smooth and with small magnitude to avoid generating severe geometric distortions in the object. After inducing the magnetic field inhomogeneity artifact we will apply the HARP tracking technique on both the original data set and the data set suffering the inhomogeneity artifact. The original data set will resemble the data set corrected by SPHERE, while the simulated data set represents the data set suffering magnetic field inhomogeneity without and then with correction. Then, we will show the effect of magnetic field inhomogeneity on HARP tracking using one-dimensional example. Then we will introduce the motion grid registration technique that tracks cardiac wall points-intersection points between vertical and horizontal tag lines- by registering the motion grid between each two successive frames.

5. RESULTS AND DISCUSSION

In the following subsections, we present the results of the set of methods required for improving cardiac wall motion tracking. First we show the effect of magnetic field inhomogeneity correction using SPHERE on cardiac wall motion tracking. In the next section we show the results of registering the simulated motion grids that models the tag lines in the cardiac wall. The data set used here is the same data set used by Osman *et al*[6]. The SPAMM tagged cardiac images was acquired using standard 1.5T scanner with software release 4.7 (General Electric Medical Systems, Milwaukee, WI). A 6 ms SPAMM pulse sequence was used to produce a tag pattern in the myocardium comprising parallel plane saturation bands separated by 5.5 mm in the image plane. A pacing lead was sewn onto the epicardial surface of the left ventricular basal free wall of a canine heart, which is used to trigger the tagging pulse sequence. The imaging sequence started 3 ms after the tagging pulses were completed. The image scanning parameters were: TR = 6.5 ms, TE = 2.1, readout bandwidth = $\pm$32 kHz, 320 mm field of view, 256 $\times$96 acquisition matrix, fractional echo, two readouts per movie frame and 6-mm slice thickness. Two sequences of 20 tagged MR short-axis images, one with horizontal tags and the other with vertical tags were acquired at 14 ms intervals during systole and breath-hold periods with segmented k-space.

5.1 Effect of magnetic field inhomogeneity on tracking

In this section, we demonstrate the effect of the magnetic field inhomogeneity in motion tracking. First we generated a simulated phase map with Gaussian extent. This phase map has been used to generate the simulated magnetic field inhomogeneity artifact in the image sequence. A point that has to be considered in the generated phase map that it has to be small in value (i.e. in the range of $\pm$0.2) which resembles the real phase map. Greater values phase maps causes geometric distortion, which is not the case in the tagged images. Generally the generated phase maps must not have a recognizable effect on the magnitude of the images yet they may change the phase. Then we applied tracking on the data set suffering the magnetic field inhomogeneity and the corrected data set to demonstrate the effect of magnetic field inhomogeneity on tracking. The effect of magnetic field inhomogeneity can be demonstrated by a dimensional example as shown in Figures 4 and 5.

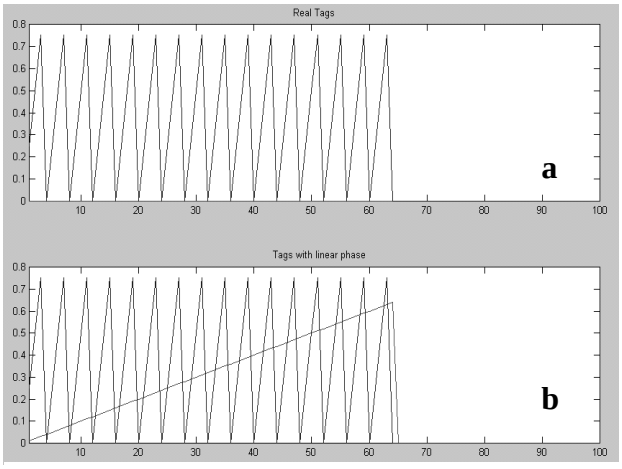

Figure 4. Two signals simulating tagged gate signal where, (a) represents a corrected real signal and (b) represents a signal suffering magnetic field inhomogeneity represented by the linear phase.

Figure 5. The change in Harmonic Phase signal due to the presence of the linear phase where (a) shows the Harmonic phase signal overlaid on the original real signal while (b) shows the Harmonic phase signal overlaid on the signal suffering inhomogeneity.

Figure 4 shows two signals simulating tagged gate signal. The difference between the two signals is that the signal in Figure 4 (a) represents a corrected real signal while in Figure 4 (b) represents a signal suffering magnetic field inhomogeneity represented by the linear phase. Figure 5 shows the change in Harmonic Phase signal due to the presence of the linear phase. Figure 5 (a) shows the Harmonic phase signal overlaid on the original real signal while Figure 5 (b) shows the Harmonic phase signal overlaid on the signal suffering inhomogeneity. The change in harmonic phase signal

from frame to another affects the tracking results by shifting the detected track points depending on the inhomogeneity values. Traditional HARP tracking made use of the magnitude of the image and discarded the phase values while magnetic field inhomogeneity correction has to be made instead for better results. We applied the magnetic field inhomogeneity in the phase encoding direction (Y-axis) in the tagged images, which affects tracking results in that direction. In order to display the images in a standardized way we rotated the images by 90 degrees such that the right ventricle should be displayed in the left part of the figure, the left ventricle to the right, and the anterior wall of the chest in the upper part. By this rotation the major effect of the magnetic field inhomogeneity will appear in the X-axis direction tracking. Figure 6 shows the values of tracked position in both X-axis direction and Y-axis direction. It is clear from the results that the error in tracking in the X-axis direction is greater than that in the Y-axis direction. Figure 7 shows the Euclidean distance error between the data set suffering inhomogeneity and the corrected data set as well as the inhomogeneity values at these tracked points.

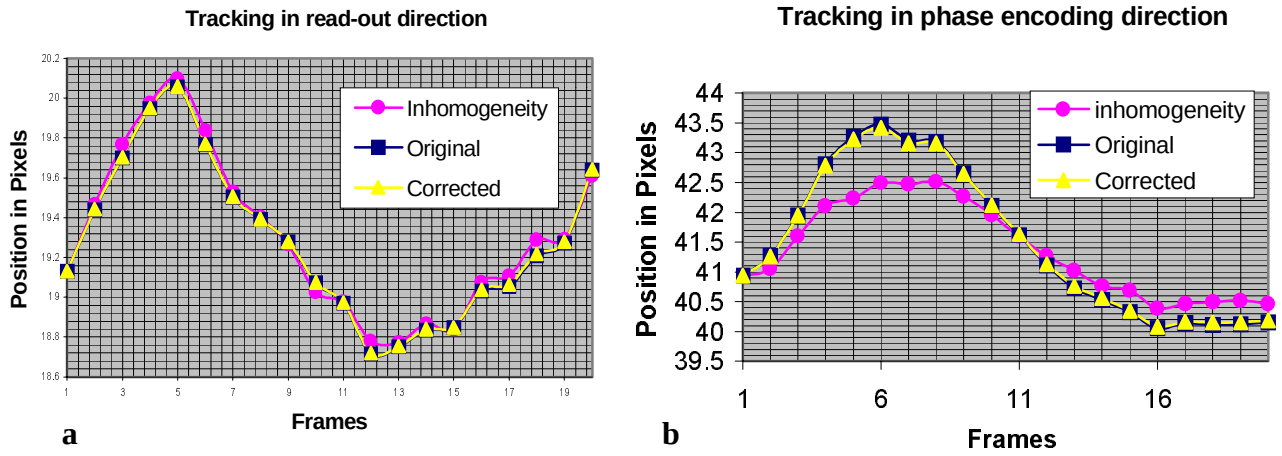

Figure 6: The values of tracked position, (a) in X-axis direction and (b)Y-axis direction. From the results the error in tracking in the X-axis direction is greater than that in the Y-axis direction.

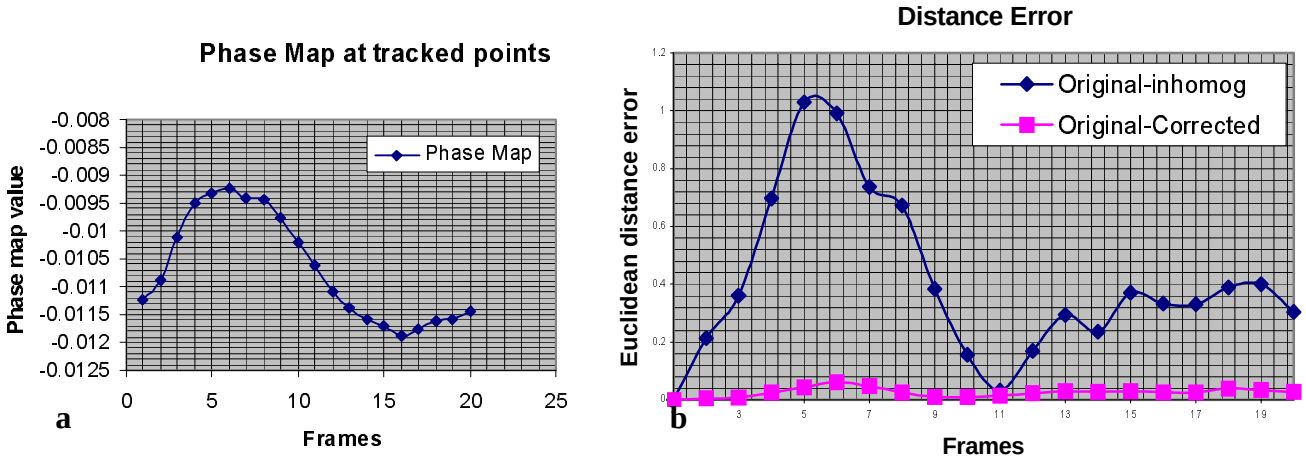

Figure 7 (a) shows the inhomogeneity values at the tracked points, while Figure 18(b) shows the Euclidean distance error between the data set suffering inhomogeneity and the corrected data.

5.2 Motion grid registration

In this section we show the results of registering the simulated motion grid with a reference grid that resembles the detected tag lines from the SPAMM tagged images. We showed in the motion grid model that our model parameters are

(c_x, c_y) and β. The first parameter will be responsible of shift (assuming rigid body motion), while β is the scaling parameter that represents the deformation in the motion grid. We generated a 33×33 reference motion grid with $\beta = 4$ and $(c_x, c_y) = (16,16)$. Figure 2 (a) shows the reference motion grid with its corresponding vertical and horizontal distance images shown in Figure 2 (b) and Figure 2 (c) respectively. The ROI was taken to be l=5,t=5,r=28 and b=28 indexes. First we will generated a motion grid that possess only transnational motion i.e. we will change (c_x, c_y) to be $(17,14)$ which means that the motion grid has been shifted inside the ROI by $(1,-2)$. Figure 8 (a) shows the generated grid with changing (c_x, c_y) only. Figure 8 (d) shows the RMS error which shows its minimum value at $(1,-2)$. Figure 9 (a) shows another generated motion grid that is shifted by $(-2,1)$ and scaled by $\beta = 5$. Figure 9 (d) shows that the minimum RMS error is exactly at the shifted center. Figure 10 (a) shows another generated motion grid that is shifted by $(-2,1)$ and scaled by $\beta = 5$ but this motion grid simulates the effect of disappearance of some tag lines due to fading of these lines during the scan or due to tissue motion that causes coincidence of these lines. Figures 10 (b) and 10 (c) show the vertical and horizontal distance images respectively suffering erroneous bright regions due to the missed tag lines. Figure 10 (d) shows that the minimum RMS error is exactly at the shifted center ensuring the robustness of the motion grid registration to the problem of disappearing tag lines.

6. CONCLUSIONS

Several factors that affect HARP-based cardiac wall motion tracking performance have been discussed. The magnetic field inhomogeneity was shown to be capable of producing phase errors that affect the performance of the technique. Such errors can be suppressed using a field inhomogeneity correction technique like SPHERE. Also, the problems of disappearing/reappearing tag lines can be addressed using a simple registration technique that estimates the correspondence of corner points in a robust manner. Further work is needed to implement and evaluate the proposed improvements in clinical practice.

ACKNOWLEDGEMENTS

We are thankful to Dr. Nael F. Osman for making his HARP programs available. We would like to acknowledge the use of the HARP data of Dr. Elliot R. McVeigh in parts of this work.

REFERENCES

1. E. A. Zerhouni, D. M. Parish, W. J. Rogers, A. Yang and E. P. Shapiro, "Human heart: tagging with MR imaging-a method for noninvasive assessment of myocardial motion," *Radiology* **169**, no. 1, pp. 59-63, 1988.
2. J. C. McEachen, II, A. Nehorai and J. S. Duncan, "Multiframe Temporal Estimation of Cardiac Nonrigid Motion," *IEEE Trans. Imag. Proc.* **9**, no. 4, pp. 651-665, April 2000.
3. J. Huang, D. Abendschein, V. G. Davila-Roman, and A. Amini, "Spatio-temporal tracking of myocardial deformations with a 4-D B-spline model from tagged MRI," *IEEE Trans. Med. Imag.* **18**, pp. 957–972, Oct. 1999.
4. P. Radeva, A. Amini, and J. Huang, "Deformable B-Solids and implicit snakes for 3-D localization and tracking of SPAMM MRI data," *Comput.Vis. Image Understandin*g **66**, no. 2, pp. 163–178, May 1997.
5. N. J. Pelc, A. Shimakawa and G. H. Glover, "Phase contrast cine MRI," *Proc. 8th Ann. SMRM*, p. 101, Amsterdam, The Netherlands, 1989.
6. N.F. Osman, W.S. Kerwin, E. R. Mc Veigh and J. L. Prince, "Cardiac Motion Tracking Using CINE Harmonic Phase (HARP) Magnetic Resonance Imaging," *Magn. Reson. Med.* **42**, pp. 1048-1060, 1999.
7. Y. M. Kadah and X. Hu, "Simulated Phase Evolution Rewinding (SPHERE): A Technique for Reducing Bo Inhomogeneity Effects in MR Images," *Magn. Reson. Med.* **38**, pp. 615-627, 1997.
8. N. Osman and J. Prince, "Direct calculation of 2D components of myocardial strain using sinusoidal MR tagging," *Proc. SPIE Med. Imag. Conf.*, San Diego, Feb. 1998.

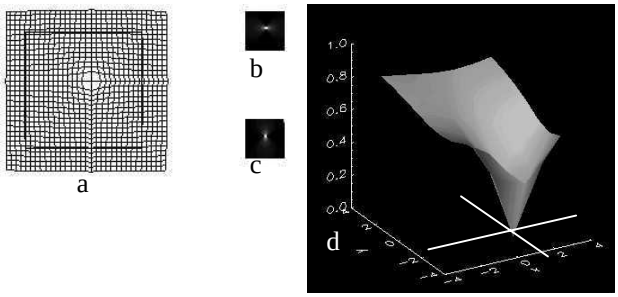

Figure 8 (a) The generated grid shifted by $(1,-2)$ and β = 4, where (b) vertical tagged distance image, (c) horizontal tagged distance image and (d) the error surface plot which shows that minimum error=0.0 at the shifted indexes values.

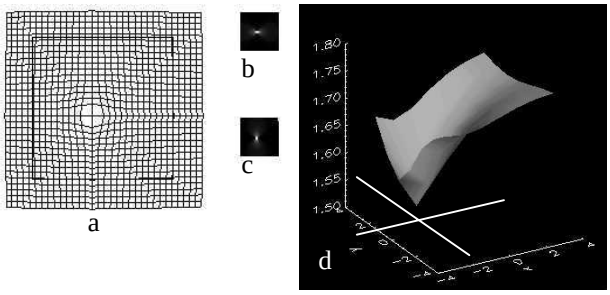

Figure 9 (a) The generated grid shifted by $(-2,1)$ and scaled by β = 5, where (b) vertical tagged distance image, (c) horizontal tagged distance image and (d) the error surface plot which shows that minimum error=1.532224 at the shifted indexes values.

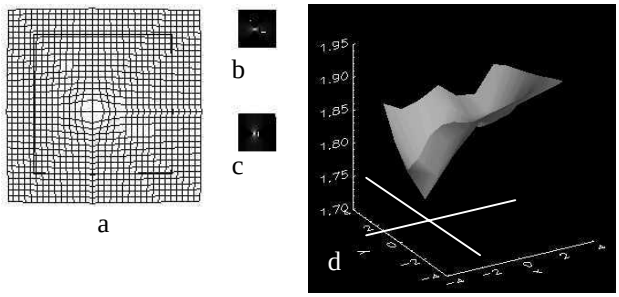

Figure 10 (a) The generated grid shifted by $(-2,1)$ and scaled by β= 5 and the grid is missing some points in both vertical and horizontal direction, where (b) vertical tagged distance image, (c) horizontal tagged distance image and (d) the error surface plot which shows that minimum error=1.739771 at the shifted indexes values.